Two-Dimensional Gas-Phase Separations Coupled to Mass Spectrometry for Analysis of Complex Mixtures

Keqi Tang, Fumin Li, Alexandre A. Shvartsburg, Eric F. Strittmatter, and Richard D. Smith*

Biological Sciences Division, Pacific Northwest National Laboratory, P.O. Box 999, Richland, Washington 99352

Ion mobility spectrometry (IMS) has been explored for decades, and its versatility in separation and identification of gas-phase ions is well established. Recently, field asymmetric waveform IMS (FAIMS) has been gaining acceptance in similar applications. Coupled to mass spectrometry (MS), both IMS and FAIMS have shown the potential for broad utility in proteomics and other biological analyses. A major attraction of these separations is extremely high speed, exceeding that of condensed-phase alternatives by orders of magnitude. However, modest separation peak capacities have limited the utility of FAIMS and IMS for analyses of complex mixtures. We report 2-D gas-phase separations that join FAIMS to IMS, in conjunction with high-resolution and accuracy time-of-flight (TOF) MS. Implementation of FAIMS/IMS and IMS/ MS interfaces using electrodynamic ion funnels greatly improves sensitivity. Evaluation of FAIMS/IMS/TOF performance for a protein mixture tryptic digest reveals high orthogonality between FAIMS and IMS dimensions and, hence, the benefit of FAIMS filtering prior to IMS/MS. The effective peak capacities in analyses of tryptic peptides are ∼500 for FAIMS/IMS separations and ∼10[6] for 3-D FAIMS/IMS/MS, providing a potential platform for ultra-high-throughput analyses of complex mixtures.

Among the greatest challenges of analytical chemistry today is characterizing samples of enormous complexity associated with systems biology research. For example, mammalian proteomes can comprise >20 000 different proteins even before counting posttranslational modifications and sequence and splicing variants.[1] A proteolytic digestion of such a mixture following standard protocols of bottom-up proteomics[1] can yield >10[6] distinct peptides and more if missed cleavage sites due to the inevitable imperfections in enzyme activity are considered. Individual peptides are commonly identified and quantified using mass spectrometry (MS).[1] However, no MS instrumentation or technique can presently characterize a significant percentage of the constituents in such a complex sample without extensive prior separations, and direct MS analyses generally identify with confidence only the most abundant proteins. "Top-down" analyses at the intact-protein level have similar limitations.

Accordingly, combinations of various separation techniques with MS have become preeminent bioanalytical technologies. The separations have conventionally been performed in condensed phases (e.g., liquid chromatography,[2] LC, or capillary electrophoresis,[3] CE, and gel techniques[4]). Single separation stages can provide peak capacities[2] of ∼10[2]−10[3]. This level is insufficient for many challenging applications: in a mixture of ∼10[6] components, a separated fraction would still comprise ∼10[3]−10[4] coeluting species on average and substantially more in some cases. Hence large-scale proteomics often involves multidimensional separations using two or more different stages, followed by MS characterization. The best-established approach involves 2-D gels,[4,5] where an isoelectric focusing (IEF) separation by isoelectric point is followed by electrophoretic (SDS−PAGE) separation by molecular size. Among liquid-phase separations, a combination of strong cation exchange LC and reversed-phase (RP) LC (in one implementation known as MudPIT[6−8]) has gained broad acceptance.[9−12] Other useful 2-D separations comprise anion exchange/RPLC,[13] size-exclusion chromatography/RPLC,[14] and other LC/LC combinations,[15] RPLC/CE,[16,17] micellar electrokinetic chromatography/ CE,[18] and CE/CE methods (e.g., IEF coupled to isotachophoresis/

(2) Shen, Y.; Zhao, R.; Berger, S. J.; Anderson, G. A.; Rodriguez, N.; Smith, R. D. *Anal. Chem.* **2002**, *74*, 4235.
(3) Shen, Y.; Xiang, F.; Veenstra, T. D.; Fung, E. N.; Smith, R. D. *Anal. Chem.* **1999**, *71*, 5348.
(4) Shevchenko, A.; Wilm, M.; Vorm, O.; Mann, M. *Anal. Chem.* **1996**, *68*, 850.
(5) Gygi, S. P.; Corthals, G. L.; Zhang, Y.; Rochon, Y.; Aebersold, R. *Proc. Natl. Acad. Sci. U.S.A.* **2000**, *97*, 9390.
(6) Washburn, M. P.; Wolters, D.; Yates, J. R. *Nat. Biotechnol.* **2001**, *19*, 242.
(7) Wolters, D. A.; Washburn, M. P.; Yates, J. R. *Anal. Chem.* **2001**, *73*, 5683.
(8) Skop, A. R.; Liu, H. B.; Yates, J.; Meyer, B. J.; Heald, R. *Science* **2004**, *305*, 61.
(9) Froehlich, J. E.; Wilkerson, C. G.; Ray, W. K.; McAndrew, R. S.; Osteryoung, K. W.; Gage D. A.; Phinney, B. S. *J. Proteome Res.* **2003**, *2*, 413.
(10) Gaucher, S. P.; Taylor, S. W.; Fahy, E.; Zhang, B.; Warnock, D. E.; Ghosh, S. S.; Gibson, B. W. *J. Proteome Res.* **2004**, *3*, 495.
(11) Shen, Y. F.; Jacobs, J. M.; Camp, D. G.; Fang, R. H.; Moore, R. J.; Smith, R. D.; Xiao, W. Z.; Davis, R. W.; Tompkins, R. G. *Anal. Chem.* **2004**, *76*, 1134.
(12) Qian, W. J.; Liu, T.; Monroe, M. E.; Strittmatter, E. F.; Jacobs, J. M.; Kangas, L. J.; Petritis, K.; Camp, D. G.; Smith, R. D. *J. Proteome Res.* **2005**, *4*, 53.
(13) Wagner, K.; Miliotis, T.; Marco-Varga, T.; Bischoff, R.; Unger, K. K. *Anal. Chem.* **2002**, *74*, 809.
(14) Opiteck, G. J.; Jorgenson, J. W.; Anderegg, R. J. *Anal. Chem.* **1997**, *69*, 2283.
(15) Evans, C. R.; Jorgenson, J. W. *Anal. Bional. Chem.* **2004**, *378*, 1952.
(16) Bushey, M. M.; Jorgenson, J. W. *Anal. Chem.* **1990**, *62*, 978.
(17) Lewis, K. C.; Opiteck, G. J.; Jorgenson, J. W.; Sheeley, D. *J. Am. Soc. Mass Spectrom.* **1997**, *69*, 2283.
(18) Rocklin, R. D.; Ramsey, R. S.; Ramsey, J. M. *Anal. Chem.* **2000**, *72*, 5244.

* To whom correspondence should be addressed. E-mail: rds@pnl.gov.
(1) Aebersold, R.; Mann, M. *Nature* **2003**, *422*, 198.

zone electrophoresis).[19] Two-dimensional approaches can provide peak capacities of $\sim 10^3 - 10^4$ for proteolytic digests.[5] Separations with additional dimensions, including combinations of methods at the intact protein and peptide level (i.e., with intermediate enzymatic digestion) can provide yet greater total peak capacities.

While 2-D condensed-phase separations are exceptionally powerful, they generally require ~ 10 h to several days[4-7] and longer if further dimensions are added. Such throughput effectively precludes many lines of biomedical research.

Physically, any separation derives from an unequal motion of different species in some medium, so the speed of condensed-phase methods is inherently limited by the achievable molecular velocities. Typical velocities in gases are higher by orders of magnitude, enabling proportionally faster separations. Thus, the need for higher throughput has focused attention on electrophoretic separations in the gas phase, which proceed $\sim 10^3 - 10^4$ times faster than those in condensed phases—on a time scale of milliseconds to seconds. These methods are ion mobility spectrometry (IMS)[20-32] and field asymmetric waveform IMS (FAIMS),[33-39] based on absolute and differential ion mobilities, respectively.

In IMS, ions travel through a fixed path inside an enclosure (typically a tube) filled with a nonreactive gas under the influence of a moderate electric field, E, created by voltages applied to surrounding electrodes. The measurement of drift velocity, v, determines the ion mobility, K:

$$K = v/E \qquad (1)$$

The raw mobility derived from eq 1 is normally converted to reduced mobility, K_0, by adjusting the buffer gas pressure (P, Torr)

and temperature (T, Kelvin) to standard conditions:

$$K_0 = K(P/760)\,(273.15/T) \qquad (2)$$

The mobility is related to orientationally averaged collision cross section $\Omega_{av}^{(1,1)}$ (rigorously the first-order collision integral) of the ion and gas molecule via the Mason–Schamp equation:[40]

$$K_0 = (3ze/16N)\,(2\pi/\mu kT)^{1/2}/\Omega_{av}^{(1,1)} \qquad (3)$$

where z is the ion charge state, N is the gas number density, μ is the reduced mass of the ion/gas molecule pair, and k is the Boltzmann constant. The quantity $\Omega_{av}^{(1,1)}$ for any collider pair can be computed using various treatments.[41-43] This capability enables structural elucidation of ions by comparing mobilities calculated for candidate geometries with measurements.[24,25,27,28,41-44]

In FAIMS, ions are separated by exploiting the dependence of ion mobility on the electric field. In pure gases, the $K(E)$ function may be expressed[36] as an infinite series:

$$K_0(E) = K_0(0)\,(1 + a(E/N)^2 + b(E/N)^4 + c(E/N)^6 + ...) \qquad (4)$$

Terms beyond $b(E/N)^4$ are generally insignificant at practical field intensities. The form of $K(E)$ in heteromolecular gases is more complex, and the FAIMS process in mixed and vapor-containing gas buffers is still not well understood.[38,39] As E increases, $K(E)$ may increase (A type ions), decrease (C type ions), or first increase and then decrease at still higher E values (B type ions).[35] This phenomenon permits separating ions by the difference between mobilities at high and low E. In FAIMS, a periodic asymmetric waveform creates a time-dependent potential $U_D(t)$ in the analytical gap between a pair of electrodes (that may form a parallel planar, coaxial cylindrical, or concentric spherical geometry). The integral of $U_D(t)$ over period is null, but time-averaged positive and negative voltages differ. This waveform pushes all ions in the gap toward one of the electrodes where they are destroyed by neutralization. Selected ion species can be prevented from drifting toward either electrode and centered in the gap by a constant compensation voltage (CV) that, when coapplied with $U_D(t)$, cancels the net ion drift due to $U_D(t)$. The CV value depends on the species, and scanning CV yields a FAIMS spectrum of the ion mixture.

IMS was introduced in 1970s as a portable economical alternative to MS for detection of airborne volatiles, e.g., environmental and industrial process contaminants, explosives, chemical warfare agents, and drugs.[20-23] Over the past decade, two major technical developments have raised and broadened the analytical importance of IMS: (i) the effective coupling of IMS to MS,[24]

(19) Mohan, D.; Pasa-Tolic, L.; Masselon, C. D.; Tolic, N.; Bogdanov, B.;Hixson, K. K.; Smith, R. D.; Lee, C. S. *Anal. Chem.* **2003**, *75*, 4432.
(20) Eiceman, G. A.; Leasure, C. S.; Vandiver, V. J. *Anal. Chem.* **1986**, *58*, 76.
(21) Hill, H. H., Jr.; Siems, W. F.; St. Louis, R. H.; McMinn, D. G. *Anal. Chem.* **1990**, *62*, A1201.
(22) Przybylko, A. R. M.; Thomas, C. L. P.; Anstice, P. J.; Fielden, P. R.; Brokenshire, J.; Irons, F. *Anal. Chim. Acta* **1995**, *311*, 77.
(23) Lopez-Avila, V.; Hill, H. H., Jr. *Anal. Chem.* **1997**, *69*, 289R.
(24) Bowers, M. T.; Kemper, P. R.; von Helden, G.; van Koppen, P. A. M. *Science* **1993**, *260*, 1446.
(25) Von Helden, G.; Wyttenbach, T.; Bowers, M. T. *Science* **1995**, *267*, 1483.
(26) Clemmer, D. E.; Hudgins, R. R.; Jarrold, M. F. *J. Am. Chem. Soc.* **1995**, *117*, 10141.
(27) Ho, K. M.; Shvartsburg, A. A.; Pan, B.; Lu, Z. Y.; Wang, C. Z.; Wacker, J. G.; Fye, J. L.; Jarrold, M. F. *Nature* **1998**, *392*, 582.
(28) Shvartsburg, A. A.; Hudgins, R. R.; Dugourd, P.; Jarrold, M. F. *Chem. Soc. Rev.* **2001**, *30*, 26.
(29) Guevremont, R.; Siu, K. W. M.; Wang, J. Y.; Ding, L. Y. *Anal. Chem.* **1997**, *69*, 3959.
(30) Hoaglund, C. S.; Valentine, S. J.; Sporleder, C. R.; Reilly, J. P.; Clemmer, D. E. *Anal. Chem.* **1998**, *70*, 2236.
(31) Lee, Y. J.; Hoaglund-Hyzer, C. S.; Srebalus Barnes, C. A.; Hilderbrand, A. E.; Valentine, S. J.; Clemmer, D. E. *J. Chromatogr., B* **2002**, *782*, 343.
(32) Collins, D. C.; Lee, M. L. *Anal. Bioanal. Chem.* **2002**, *372*, 66.
(33) Buryakov, I. A.; Krylov, E. V.; Nazarov, E. G.; Rasulev, U.K. *Int. J. Mass Spectrom. Ion Processes* **1993**, *128*, 143.
(34) Buryakov, I. A. *Talanta* **2003**, *61*, 369.
(35) Purves, R. W.; Guevremont, R.; Day, S.; Pipich, C. W.; Matyjaszczyk, M. S. *Rev. Sci. Instrum.* **1998**, *69*, 4094.
(36) Guevremont, R.; Barnett, D. A.; Purves, R. W.; Viehland, L. A. *J. Chem. Phys.* **2001**, *114*, 10270.
(37) Guevremont, R. *J. Chromatogr., A* **2004**, *1058*, 3.
(38) Eiceman, G. A.; Krylov, E. V.; Krylova, N. S.; Nazarov, E. G.; Miller, R. A. *Anal. Chem.* **2004**, *76*, 4937.
(39) Shvartsburg, A. A.; Tang, K.; Smith, R. D. *Anal. Chem.* **2004**, *76*, 7366.

(40) Mason, E. A.; McDaniel, E. W. *Transport Properties of Ions in Gases*; Wiley: New York, 1988.
(41) Shvartsburg, A. A.; Jarrold, M. F. *Chem. Phys. Lett.* **1996**, *261*, 86.
(42) Mesleh, M. F.; Hunter, J. M.; Shvartsburg, A. A.; Schatz, G. C.; Jarrold, M. F. *J. Phys. Chem.* **1996**, *100*, 16082.
(43) Shvartsburg, A. A.; Liu, B.; Siu, K. W. M.; Ho, K. M. *J. Phys. Chem. A* **2000**, *104*, 6152.
(44) Jackson, K. A.; Horoi, M.; Chaudhuri, I.; Frauenheim, T.; Shvartsburg, A. A. *Phys. Rev. Lett.* **2004**, *93*, # 013401.
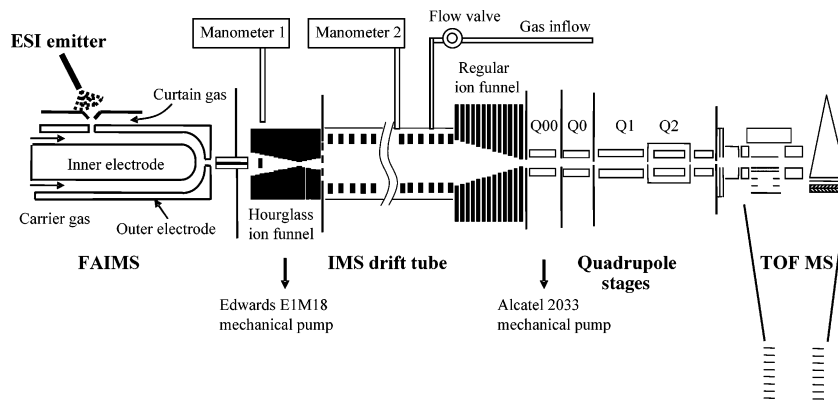
Figure 1. Schematic of the ESI-FAIMS/IMS/Q-TOF MS instrumentation.

especially the advent of IMS/TOF instrumentation that enables a parallel dispersion of ion mixtures in mobility and mass/charge (m/z) dimensions,[29,30] and (ii) interfacing of ESI and MALDI soft ionization sources to IMS[45] and IMS/MS,[25,28] which has enabled many biomedical applications. Similarly for FAIMS, coupling to MS and ESI-MS[35] has opened a range of environmental and biological applications.[37]

While FAIMS and IMS are extremely fast, their resolving power is limited: typically ~10−30 for FAIMS[46] and ~50−200 for IMS.[47−50] These values are obviously too low for complex biological mixtures, especially since IMS is only partially orthogonal to MS, and thus, the useful peak capacity of IMS/MS is less than the product of individual IMS and MS peak capacities.[51,52] The total peak capacity can be increased by adding a condensed-phase separation (e.g., RPLC) prior to FAIMS[53] or IMS.[31,54] While this hybrid 2-D strategy has merits, invoking a condensed-phase stage necessarily decreases the throughput significantly. It also restricts the analyte matrixes to those compatible with the condensed-phase technique, a well-known limitation of LC/ESI-MS.

Here we report the first gas-phase ion separations in two dimensions, achieved by joining FAIMS and IMS stages followed by TOF MS, and demonstrate the utility of FAIMS/IMS/MS for high-throughput analyses of complex mixtures.

EXPERIMENTAL METHODS

Key Features of the IMS/MS Platform with Ion Funnel Interfaces. The new ESI-FAIMS/IMS/MS system (Figure 1) was constructed using a previously described IMS/MS platform.[55,56] Concisely, it consists of an IMS drift tube and a TOF MS interfaced using an electrodynamic ion funnel.[57] The drift tube is a modular assembly of identical units, which provides a variable IMS length and ease of construction.[56] Each unit comprises a housing with a stack of ring electrodes inside and vacuum flanges on both ends. Units are electrically insulated from each other by spacers and vacuum-sealed on O-rings. All IMS electrodes are consecutively connected via a resistor chain. The median ring of each unit is electrically shorted to its chamber, to minimize the voltage difference between any adjacent surfaces inside the IMS. This maximizes the IMS operating voltage achievable without electrical breakdown of the buffer gas. The present design includes 10 units with total length of 210 cm; further lengthening by adding units is straightforward.[56] The drift voltage is generated by a high-voltage power supply and monitored by a custom probe. That voltage is applied to the first electrode and equally partitioned across the drift tube by a resistor chain. The drift tube is continuously filled with buffer gas, here dry N_2. The pressure inside is controlled by a valve and monitored using the two capacitance manometers on the drift tube and preceding source chamber (Figure 1).

Ion packets separated by IMS are analyzed by a Q-TOF (Sciex Q-Star) modified by removal of curtain gas−orifice interface and the addition of a small differentially pumped chamber Q00, housing a short quadrupole (Figure 1). This stage is needed to maintain a low gas pressure in the next collisional cooling quadrupole (Q0), else excessive ion transit times through that region would degrade the IMS separation.[56] The IMS and TOF pulsing sequences are integrated under the command of custom software that provides overall instrument control. This utility also receives data streaming from the TDC, converts them into 2-D IMS/MS frames, and makes histograms of those into final IMS/MS maps.

The principal design feature is an ion funnel at the IMS terminus with the acceptance orifice approximately matching the IMS electrode aperture. The funnel consists of a stack of ring

(45) Wittmer, D.; Chen, Y. H.; Luckenbill, B. K.; Hill, H. H., Jr. *Anal. Chem.* **1994**, *66*, 2348.
(46) Shvartsburg, A. A.; Tang, K.; Smith, R. D. *J. Am. Soc. Mass Spectrom.* **2005**, *16*, 2.
(47) Dugourd, Ph.; Hudgins, R. R.; Clemmer, D. E.; Jarrold, M. F. *Rev. Sci. Instrum.* **1997**, *68*, 1122.
(48) Wu, C.; Siems, W. F.; Asbury, G. R.; Hill, H. H., Jr. *Anal. Chem.* **1998**, *70*, 4929.
(49) Srebalus, C. A.; Li, J.; Marshall, W. S.; Clemmer, D. E. *Anal. Chem.* **1999**, *71*, 3918.
(50) Asbury, G. R.; Hill, H. H., Jr. *J. Microcolumn. Sep.* **2000**, *12*, 172.
(51) Shvartsburg, A. A.; Siu, K. W. M.; Clemmer, D. E. *J. Am. Soc. Mass Spectrom.* **2001**, *12*, 885.
(52) Ruotolo, B. T.; Gillig, K. J.; Stone, E. G.; Russell, D. H. *J. Chromatogr., B* **2002**, *782*, 385.
(53) Venne, K.; Bonneil, E.; Eng, K.; Thibault, P. *Anal. Chem.* **2005**, *77*, 2176.
(54) Myung, S.; Lee, Y. J.; Moon, M. H.; Taraszka, J.; Sowell, R.; Koeniger, S.; Hilderbrand, A. E.; Valentine, S. J.; Cherbas, L.; Cherbas, P.; Kaufmann, T. C.; Miller, D. F.; Mechref, Y.; Novotny, M. V.; Ewing, M. A.; Sporleder, C. R.; Clemmer, D. E. *Anal. Chem.* **2003**, *75*, 5137.

(55) Smith, R. D.; Tang, K.; Shvartsburg, A. A. U.S. Patent 6,818,890, 2004.
(56) Tang, K.; Shvartsburg, A. A.; Lee, H. N.; Prior, D. C.; Buschbach, M. A.; Li, F.; Tolmachev, A. V.; Anderson, G. A.; Smith, R. D. *Anal. Chem.* **2005**, *77*, 3330.
(57) Kim, T.; Tolmachev, A. V.; Harkewicz, R.; Prior, D. C.; Anderson, G. A.; Udseth, H. R.; Smith, R. D.; Bailey, T. H.; Rakov, S.; Futrell, J. H. *Anal. Chem.* **2000**, *72*, 2247.

electrodes carrying an axial dc gradient, with opposite phases of a harmonic rf potential coapplied to neighboring electrodes.[57] The ring apertures narrow along the stack, in the direction of ion motion through the funnel. Then ion packets entering the ion funnel are propelled axially by the dc field, while confined radially by the rf field. Ion funnels were extensively evaluated in various ESI-MS interfaces at ~1−10 Torr pressure and proven to radially compress ion beams while providing a near 100% ion transmission over a broad m/z range.[57,58] At API−MS interfaces, the gas dynamics caused by abrupt pressure drop from 1 atm to a few Torr limits the conditions for effective rf focusing in the funnel. The gas dynamics at IMS terminus is relatively insignificant, because (i) the pressure drop from IMS to MS is ~2 orders of magnitude lower than that from API to MS and (ii) the funnel precedes the drop instead of being in the turbulent region after it. Therefore, an ion funnel should be yet more effective at the IMS/MS interface. The present configuration achieves essentially perfect transmission through the IMS and into MS, even for IMS as long as 210 cm.[56] Crucially, ion focusing in the funnel does not affect the IMS separation, in terms of either resolution or absolute mobility measured.[56]

Ions arriving from the source are conveyed into IMS by another ion funnel. Unlike those at API−MS interfaces elsewhere,[57,58] the funnel leading to IMS must deliver discrete ion packets. With a continuous ion source such as ESI or ESI-FAIMS, high ion utilization requires an effective accumulation of ions between IMS pulses and their swift ejection into the drift tube, which calls for a substantial ion storage volume. Hence, the funnel at IMS entrance is of the novel "hourglass" shape, with the conductance limit to IMS in the middle followed by a volume of several cubic centimeters where ions are parked behind a mesh while the IMS gate is closed.[55,56] The funnel features a jet disrupter that suppresses the turbulent gas flows hindering rf ion focusing.[55,56,59]

FAIMS/IMS Arrangement. The previous IMS/MS platform[55,56] summarized above was augmented by a FAIMS stage between the ESI source and IMS, enabling 2-D FAIMS/IMS separations. The FAIMS (Selectra, Ionalytics, Ottawa, Canada) was modified as described below. It comprises the electrode set effecting ion separation and the power unit that supplies requisite asymmetric waveform, including $U_D(t)$ (the sum of 0.75 and 1.5 MHz harmonics with 2:1 amplitude ratio) and CV, to the electrodes. The two electrodes are arranged in the coaxial cylinder geometry with a hemispherical terminus.[37,60] In the cylindrical region, the analytical gap width (g_C) is 2 mm, defined by the internal electrode of o.d. = 16 mm and external electrode of i.d. = 20 mm. At the terminus, g_H may be varied from 1.7 to 2.7 mm in 0.1-mm increments by translation of the inner electrode.[61] This provides control of the FAIMS resolution that can be increased at the cost of sacrificing analytical sensitivity.[46,61] Similarly to Guevremont et al.,[61] we find the FAIMS sensitivity and resolution to maximize at g_H = 2.0 mm and 2.5−2.6 mm, respectively, but the ion signal at $g_H \geq$ 2.5 mm is quite low. As a compromise, all measurements reported here are for g_H = 2.3 mm.

Ions are generated using a nano-ESI emitter made by pulling sections of fused-silica capillary (50-μm i.d./150-μm o.d., Polymicro Technologies, Phoenix, AZ) with a butane torch. Samples are infused at 0.4 μL/min by a microsyringe driven by a syringe pump (kd Scientific, Holliston, MA). The emitter is mechanically adjustable with respect to the ion inlet on the side of outer FAIMS electrode. The inlet uses a gas curtain−orifice design, where ions are desolvated in a counterflow of dry N_2 while pulled into the sampling orifice by an electric field. Another stream of the same gas carries desolvated ions along the analytical gap through FAIMS. The total gas flow is regulated by the flow controller at 2 L/min.

Separations in FAIMS may utilize various gas buffers, with the choice strongly affecting the outcome.[39,62] Most early work has employed pure gases (primarily air or N_2), but FAIMS resolution and sensitivity often improve in gas mixtures where high-field ion mobilities exhibit a strong non-Blanc behavior.[39,63] In particular, the 1:1 He/N_2 mixture has proven a good choice for most analytes including protein digests[39,53,63,64] and is used here.

The outer FAIMS electrode is coupled to the capillary inlet (0.43-mm i.d.) into hourglass ion funnel (Figure 1) using a custom peek adapter, with an ~0.5-mm air gap left for electrical insulation and to permit the outflow of excess FAIMS gas. Since the ions generated in ESI are already desolvated when injected into FAIMS and further by field heating inside, the capillary need not be heated and is held at room temperature.

All the components preceding the IMS, including both the Selectra electrodes and power supply, are electrically floated on the IMS drift voltage.[65] This was implemented by floating all relevant ac and dc power supplies, with the high-voltage ac input supplied by an isolation transformer.[56] Since the (grounded) control PC cannot communicate with a floated FAIMS via electrical cables, those were replaced by optical cables.[65] For electrical isolation and safety reasons, the FAIMS power unit is enclosed in an insulating container secured inside a grounded metal cage surrounding the entire ESI-FAIMS/IMS system. Referenced to the floating voltage, the typical dc potentials on elements preceding IMS are as follow: ESI needle (~2.0 kV), capillary (200 V), funnel entrance aperture (190 V), jet disrupter (~170 V), and funnel exit aperture (40 V). These values are somewhat lower than those in the ESI-IMS/MS platform,[56] because of the upper limit on Selectra electrode bias. Accordingly, the dc field in the funnel decreases to ~15 V/cm, well within the operational range. As the IMS gate voltages in "open" and "closed" states must bracket the bias of last funnel plate, those were also reduced to 25 and 52 V, respectively. All above voltages are for positive ions and should be reversed for negative ion analyses. The voltages on elements of IMS and IMS/MS ion funnel remain as in the earlier ESI-IMS/MS platform.[56]

Instrumental Evaluation Procedure. The performance of the ESI-FAIMS/IMS/MS system was tested using a digest of a

(58) Belov, M. E.; Gorshkov, M. V.; Udseth, H. R.; Anderson, G. A.; Smith, R. D. *Anal. Chem.* **2000**, *72*, 2271.
(59) Kim, T.; Tang K.; Udseth, H. R.; Smith, R. D. *Anal. Chem.* **2001**, *73*, 4162.
(60) Guevremont, R.; Purves, R. *J. Am. Soc. Mass Spectrom.* **2005**, *16*, 349.

(61) Guevremont, R.; Thekkadath, G.; Hilton, C. K. *J. Am. Soc. Mass Spectrom.* **2005**, *16*, 948.
(62) Barnett, D. A.; Ells, B.; Guevremont, R.; Purves, R. W.; Viehland, L. A. *J. Am. Soc. Mass Spectrom.* **2000**, *11*, 1125.
(63) Barnett, D. A.; Ells, B.; Guevremont, R.; Purves, R. W. *J. Am. Soc. Mass Spectrom.* **2002**, *13*, 1282.
(64) McCooeye, M.; Ding, L.; Gardner, G. J.; Fraser, C. A.; Lam, J.; Sturgeon, R. E.; Mester, Z. *Anal. Chem.* **2003**, *75*, 2538.
(65) Tang, K.; Shvartsburg, A. A.; Smith, R. D. U.S. patent pending.

**Table 1. Sample Used for FAIMS/IMS/MS Evaluation[a]**

proteins and peptides	Catalog No.#	concn
bovine serum albumin	A7368	0.195
bovine carbonic anhydrase	C3934	0.200
bovine β-lactoglobulin	L3908	0.196
bovine serotransferrin	T1408	0.194
rabbit glyceraldehyde-3-phosphate dehydrogenase	G2267	0.198
E. coli β-galactosidase	G5635	0.204
bovine α-lactalbumin	L6010	0.195
equine skeletal muscle myoglobin	M0630	0.200
chicken ovalbumin	A2512	0.198
bovine cytochrome c	C2037	0.198
rabbit phosphorylase b	P6635	0.198
bradykinin fragment 2−9	B1901	0.003
des pro ala bradykinin	B4791	0.018
bradykinin	B3259	0.048
try bradykinin acetate salt	B4764	0.012
fibrinopeptide A	F3254	0.006
tyr c peptide	C9781	0.018
osteocalcin fragment 7−19 human	O3632	0.006
syntide 2	S2525	0.028
leptin fragment 93−105 human	L7288	0.015
[ala92]-peptide 6	P7967	0.008
ProteoMassäP14R MALDI-MS standard	P2613	0.005
vasoactive intestinal peptide fragment 1−12 human	V0131	0.014
diazepam binding inhibitor	G9898	0.009
epidermal growth factor receptor fragment 661−681	E9520	0.006
3X FLAGpeptide	F4799	0.003
presenilin-1 N-terminal peptide	P2490	0.214
dynorphin A porcine fragment 1−13	D7017	0.062
neurotensin	N6383	0.017
angiotensin	A9650	0.024

[a] Components, Sigma catalog no., and final concentrations of peptides and protein digests (mg/mL). Digested proteins are in boldface type.

pool of 11 common proteins (covering the mass range of 11−116 kDa that is representative of typical proteomes) mixed with 19 typical peptides (Table 1). The protein mixture was denatured in urea and thiourea, reduced by dithiothreitol, diluted 10× in 100 mM ammonium bicarbonate, and digested by trypsin (Promega, Madison, WI) in a 1:50 enzyme/protein ratio. Ideally, this would produce 401 tryptic peptides. The digest was cleaned using a C_{18} SPE column (Supelco, Bellefonte, PA), combined with a solution of 19 peptides, and dissolved in 50:49:1 methanol/deionized water/ acetic acid to the concentrations listed in Table 1. All peptides and proteins used are available from Sigma (Table 1), and solvents are HPLC grade (Fisher Scientific).

The experimental sequence is illustrated in Figure 2. First, an ion mixture is separated in FAIMS dimension only by Selectra operated in the CV scan mode (at the speed of 5 V/min), with IMS in the continuous transmission regime (entrance gate permanently open).[56] This yields a CV spectrum usual for FAIMS/ MS experiments.[37] Then IMS is switched to regular operation (gate opened periodically to release ion packets), and a sequence of 2-D IMS/MS maps is acquired with Selectra stepping through a number of designated CVs with set dwell times (Figure 2). Here, the whole CV range revealed in FAIMS is traversed with an ~1-V increment. In the end, the experiment yields a data set in three dimensions: CV, drift time, and m/z.

The upper limit of measurable m/z range (in any mode) is proportional to the TOF cycle period squared, but faster cycling
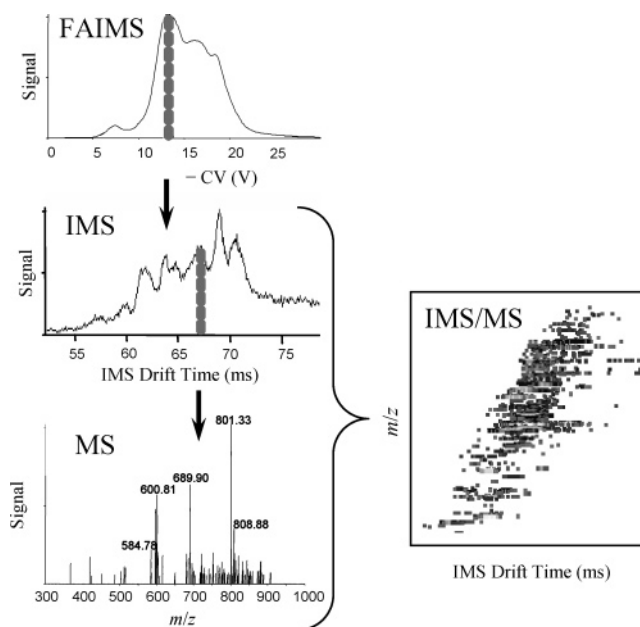
Figure 2. Diagram of the FAIMS/IMS/MS experimental sequence.

improves the throughput and ion utilization efficiency. So one would choose the shortest period that still covers the full m/z range of analyzed ion mixture. The highest m/z observed with the present sample is ~1100, a period of 100 μs corresponds to m/z up to ~1140. Some data were acquired with a 143-μs period that reveals m/z up to ~2200, to ensure that higher m/z species were not missed.

The gas pressure in IMS was 4.00 ± 0.03 Torr. To maintain the buffer composition in IMS (N_2) differing from that in FAIMS (1:1 He/N_2), a gas flow out of the drift tube toward the ion source is critical.[56] This is ensured by keeping the pressure in the inlet funnel slightly (~30 mTorr) below that in IMS.[56] The IMS pulsing period is generally set beyond the longest drift time of any analyte (here ~100 ms), else ions originating from different pulses may mix in the drift tube. However, when all species present have mobilities (and thus drift times) within a known limited range as happens for tryptic peptide ions generated by ESI, the throughput and sensitivity may be raised by multiplexing ion packets in the drift tube. This is employed here to a modest extent, with IMS periods of 50 ms. To avoid a peak broadening in IMS, the injection pulse should be significantly shorter than the greater of diffusional peak width and detector channel width (i.e., the TOF cycle period).[66] Considering that the diffusional peak width in these experiments was ~0.5−1 ms and the TOF period was <0.14 ms, we chose the pulse duration of 0.1 ms. Under present conditions, the IMS resolving power is ~100 for singly charged ions.[56]

RESULTS

Characteristics of FAIMS/IMS/MS Measurements. Peptides of all charge states behave as C-type ions in FAIMS with either N_2 or 1:1 He/N_2 buffer[53,63] and thus are analyzed in the "P2" mode where both the dispersion voltage (DV) and CV are negative.[35] Here we use DV = −4 kV, the maximum DV amplitude available, which typically provides the best separations. The CV

(66) Rokushika, S.; Hatano, H.; Baim, M. A.; Hill, H. H., Jr. *Anal. Chem.* **1985**, *57*, 1902.
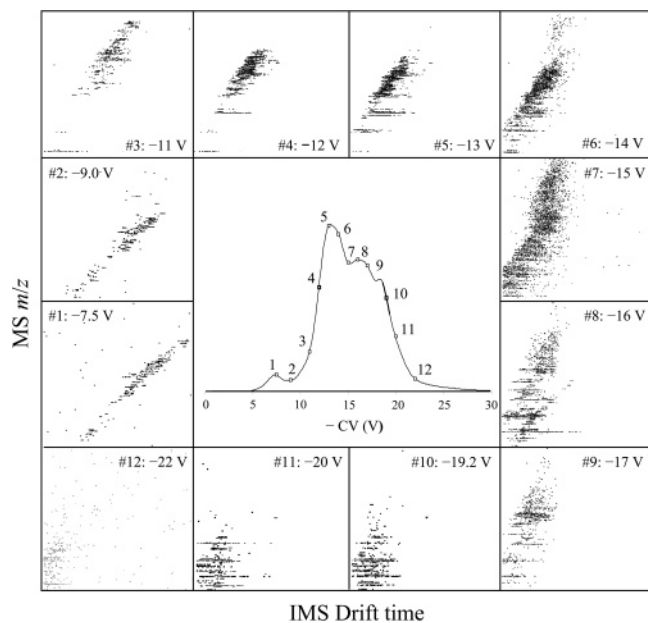
Figure 3. FAIMS CV spectrum for the test analyte mixture (central panel), and IMS/MS maps at 12 (out of 16 measured) CV values across the spectrum, as labeled (panels 1−12). All maps are for IMS drift times of 50−100 ms (horizontal axes) and m/z of 400−1200 (vertical axes). The four maps not shown were acquired at CV = −12.2, −12.5, −17.5, and −20.8 V.
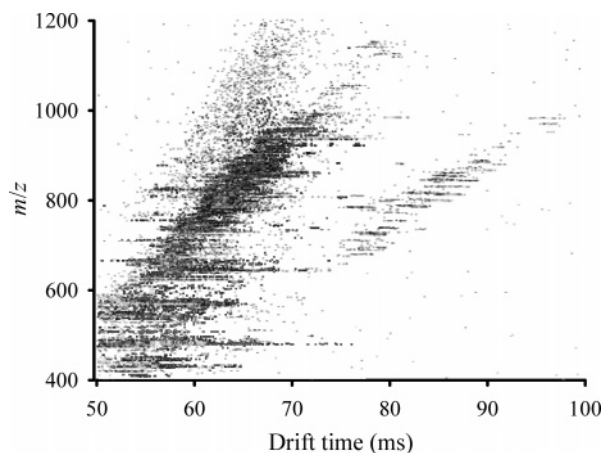

Figure 4. Summary IMS/MS map of test analyte compiled from CV-selected maps.

spectrum obtained under these conditions is shown in Figure 3. The spectrum spans the {−6 V; −28 V} range, in agreement with findings for other tryptic digests: {−7 V; −35 V} for a mixture of 13 proteins[63] and {−8 V; −25 V} for that of another 8 proteins.[53]

The CV-selected IMS/MS maps were obtained for 16 CVs between −7.5 and −22 V−the range of FAIMS spectrum with significant intensity (Figure 3). Agglomeration of these maps creates a global IMS/MS map that is typical of tryptic digests in ESI/IMS/TOF studies (Figure 4).[49,54] All 16 maps were processed to distinct spots that correspond to different ions, with charge states determined from the MS isotopic pattern. We found ∼10−70 spots per map depending on signal intensity at a particular CV, with at least ∼360 unique spots out of >600 total (Figure 5). By general location of spots, the maps in Figure 3 fall into three groups: I for |CV| of <10 V, II for ∼11−17 V, and III for >18 V. Virtually all peptides in group I (∼100 unique spots) have $z = 1$,
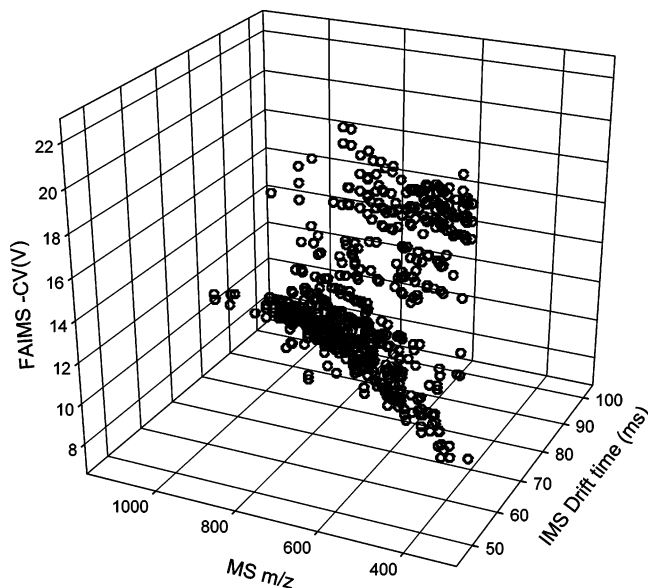

Figure 5. Dispersion of distinct peptide spots identified in 3-D FAIMS/IMS/MS space.

while in II (∼200 unique spots) and III (∼60 unique spots) most have $z = 2$ and some have $z = 3$. This pattern is consistent with the known charge-state separation of peptides in FAIMS.[53,63,67]

As tryptic peptides with $z = 1$ and $z \geq 2$ occupy different parts of the IMS/MS separation space,[49,54] naturally the maps of groups I and II grossly differ (Figure 3). This might suggest that FAIMS prefractionates species that would be distinguished in IMS anyway, i.e., that FAIMS and IMS separations are not orthogonal. If this were true, adding FAIMS to IMS/MS would serve no purpose. To understand this crucial issue, one should compare the actual spots in maps within each group. For example, maps 1 and 2 of group I (Figure 3) contain 71 and 47 distinct ions, respectively. These spots occupy essentially the same separation space in the two maps. This is not surprising as, with any IMS buffer gas, the standard deviation of representative singly charged tryptic peptides from the linear regression in IMS/MS graphs[51,52,68] is ∼3−3.5%, with extreme deviations of ∼10%. (Combined data from maps 1 and 2 exhibit similar statistics.) However, only 10 out of 118 total spots coincide within (liberally expanded) 2-D error margin of IMS/MS measurement and hence *may be* common to both maps (Figure 6). Similarly, spots in maps 6 and 9 of group II for doubly charged peptides cover nearly the same area (Figure 3). However, none of the spots identified in map 9 is found in map 6 (Figure 6). These results clearly bear out the analytical benefit of FAIMS filtering prior to IMS/MS analyses.

The selection of CVs depends on experimental priorities. First, one may seek to cover the whole CV spectrum or focus on a specific range, e.g., that encompassing doubly charged peptide ions.[53] Second, one may choose a denser CV sampling grid for maximum coverage or a sparser one for higher throughput. A low overlap between the spots in some IMS/MS maps of the same group raises the question of CV grid density needed for good coverage. Maps 6 and 9 with zero overlap differ by 3.0 V in CV,

(67) Guevremont, R.; Barnett, D. A.; Purves, R. W.; Vandermey, J. *Anal. Chem.* **2000**, *72*, 4577.
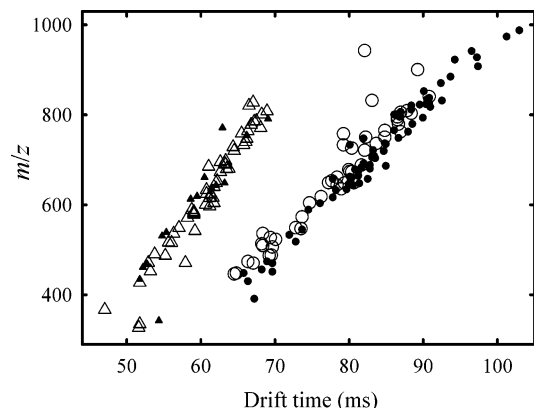(68) Ruotolo, B. T.; McLean, J. A.; Gillig, K. J.; Russell, D. H. *J. Mass Spectrom.* **2004**, *39*, 361.

Figure 6. Distinct species identified in selected IMS/MS maps of group I (circles, empty for CV = −7.5 V and filled for −9 V) and group II (triangles, empty for CV = −14 V and filled for −17 V).

and maps 1 and 2 with 8% overlap differ by 1.5 V. As expected, maps at more closely spaced CVs have a more similar content: the fraction of shared spots increases to ~60% for a difference of 1 V (maps 6 and 7), ~85% for 0.75 V (e.g., maps 10 and 11), and ~95% for 0.2 V (maps not shown). Hence, 1 V is a reasonable CV step, though a slightly denser grid may be desired to ensure complete sample coverage and define the CV for each species more precisely.

For maximum coverage, the CV step should be somewhat smaller than full width at half-maximum (fwhm) of CV peaks for individual ions. Generally the peaks in a CV spectrum broaden at higher absolute CV.[69] For example, mean fwhm and standard deviations in present FAIMS data at CV = −7.5, −13, and −20.5 V are respectively 0.65 ± 0.15, 1.1 ± 0.15, and 2.5 ± 0.7 V: fwhm roughly scales with |CV|. (Absolute values should not be compared to previous reports[63] because of different FAIMS geometries.) The peak broadening at higher |CV| increases the correlation between IMS/MS maps measured at equal CV spacing; e.g., maps at CV of −19.2 and −20.7 V share ~65% of spots versus ~10% in maps at −7.5 and −9 V that also are 1.5 V apart. A more sophisticated strategy would be to use CV step sizes that vary with CV in proportion to the typical fwhm of the ions of interest. In particular, a constant relative CV step could be employed.

Orthogonality between FAIMS and IMS and the Overall Peak Capacity of Separations. To explore the orthogonality between dimensions of FAIMS/IMS/MS further, we collapsed the 3-D plot in Figure 5 onto constituent 2-D planes. The projection on the IMS/MS plane showing a clear separation of singly and multiply charged peptides along different trend lines (Figure 4) is well known.[49,54] The projection on the FAIMS/MS plane (Figure 7a) is also similar to previous findings[53,63,67] and shows essentially no correlation between CV and m/z values. Separations in the FAIMS and IMS dimensions are also substantially independent (Figure 7b), though there is a modest correlation as peptides with $z = 1$ tend to have both lower mobility and lower |CV| than those with $z \geq 2$. It remains to be seen whether that correlation is general or specific to peptides. Regardless, there is no obvious correlation for ions of any particular charge state, including $z = 1$.

Fundamentally, IMS and FAIMS should be substantially orthogonal: IMS measures mobility while FAIMS measures its derivative with respect to electric field, and a function and its derivative are not *a priori* correlated. This expectation was supported by comparison of FAIMS and IMS data for a limited set of peptide ions.[67] Experiments combining FAIMS with energy-loss measurements led to the same inference[70,71] and also suggested a similar orthogonality between FAIMS and IMS for intact proteins.[71] This work shows that orthogonality directly and harnesses it to boost the overall peak capacity and specificity obtainable using gas-phase separations.

The peptides studied here were spread over a CV space of ~20−25 V, with the mean peak fwhm of ~1−1.5 V. Hence, the FAIMS peak capacity is ~15−20. The IMS separation space occupied *at any CV* is ~20−30 ms, and thus, the effective peak capacity (given the present IMS peak width of ~0.6−1 ms) is ~30. Therefore, the FAIMS/IMS 2-D peak capacity (adjusted for the correlation between two dimensions) is ~500, which is comparable to high-quality 1-D LC separations requiring several hours.[2] In contrast, a FAIMS/IMS analysis may (if signal intensity is sufficient) be completed within a single FAIMS scan that, for a CV range of 25 V, may require less than 1 min. Indeed, in 50 s one can step through 25 CV values with 1-V increments and 2-s dwell times, acquiring 40 elementary IMS/MS frames during each (i.e., using 50-ms IMS period). This suggests the possibility of an orders of magnitude acceleration of analyses using FAIMS/IMS/MS compared to LC/MS.

CONCLUSIONS

We have developed and demonstrated two-dimensional gas-phase ion separations prior to MS by combining FAIMS and IMS. The desirability of such a combination has been previously noted,[67,72,73] but coupling FAIMS to IMS/MS has been impractical because of low sensitivity arising from a combination of relatively low duty cycle of FAIMS (due to its filtering nature), significant ion losses at the ESI/IMS interface, and additional major losses (>90% and often >99%) at the IMS/MS junction.[56] The present FAIMS/IMS is integrated and interfaced to MS using ion funnels that provide an essentially lossless ion transmission from the IMS drift tube to the MS.[56] This potentially raises the sensitivity of FAIMS/IMS/MS to that of FAIMS/MS without IMS.

The present ESI-FAIMS/IMS/MS peptide analyses show a substantial orthogonality between FAIMS and IMS separations, thus establishing the value of adding a FAIMS prior to IMS/MS. The 2-D FAIMS/IMS peak capacity for tryptic peptides is ~500, which is comparable with high-quality condensed-phase separations that are orders of magnitude slower. With the present TOF MS peak capacity of ~10^4, assuming only 20% independence between IMS and MS dimensions, the 3-D FAIMS/IMS/MS peak capacity is ~$500 \times 0.2 \times 10^4 = 10^6$. Even higher peak capacities, conservatively 1000−1500 for FAIMS/IMS and ~5×10^6 for FAIMS/IMS/MS, would be feasible using an IMS with the

(69) Shvartsburg, A. A.; Tang, K.; Smith, R. D. *J. Am. Soc. Mass Spectrom.* **2004**, *15*, 1487.

(70) Purves, R. W.; Barnett, D. A.; Ells, B.; Guevremont, R. *Rapid Commun. Mass Spectrom.* **2001**, *15*, 1453.

(71) Purves, R. W.; Barnett, D. A.; Ells, B.; Guevremont, R. *J. Am. Soc. Mass Spectrom.* **2000**, *11*, 738.

(72) Guevremont, R. *Can. J. Anal. Sci. Spectrosc.* **2004**, *49*, 105.

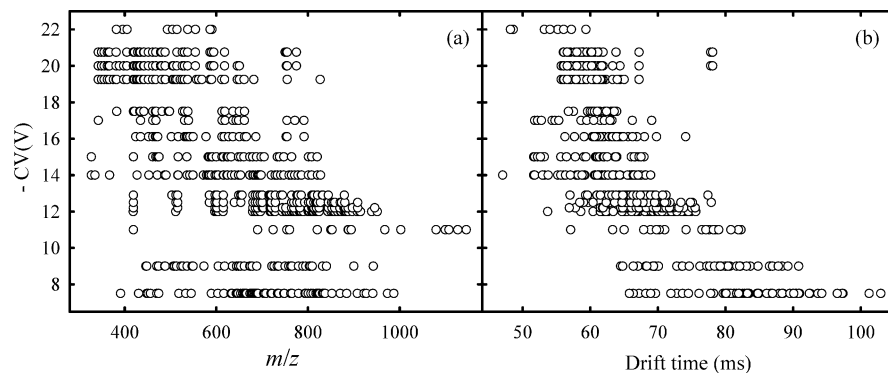(73) Guevremont, R.; Purves, R.; Barnett, D. U.S. Patent Application 2003/0089847 A1.

Figure 7. Dispersions of distinct peptide spots in the FAIMS/MS (a) and FAIMS/IMS (b) planes confirming the orthogonality of FAIMS separations to MS and IMS.

maximum reported resolving power (>150 for singly charged ions[47−50]) or a FAIMS with somewhat higher resolution (e.g., achieved via mechanical or operational modifications[46] or analyte-specific optimization of buffer gas composition[38,39]) in conjunction with the higher MS resolution obtainable from state-of-the-art orthogonal TOF instrumentation.

Tryptic peptide ions derived from ESI constitute a set of low chemical and structural diversity spanning a limited *m/z* range. More diverse mixtures (e.g., including metabolites, nucleotides, lipids, or whole proteins) inhabit a broader separation space in both their FAIMS and IMS dimensions,[74,75] resulting in peak capacities up to ~4000 for FAIMS/IMS (~25 for FAIMS × ~160 for IMS) and ~$(2-3) \times 10^7$ for FAIMS/IMS/TOF. Thus, the utility of the FAIMS/IMS/MS platform extends to applications well beyond bottom-up proteomics, e.g., characterization of gas-phase macromolecular conformations (to be described elsewhere).

Finally, the FAIMS/IMS combination does not have to be coupled to MS, but may be operated with a Faraday cup or other detector, as in existing stand-alone FAIMS or IMS devices. The advantage of FAIMS/IMS over either FAIMS or IMS in achievable resolution and peak capacity will allow addressing many specificity challenges faced by present FAIMS or IMS analyses (e.g., for detection of volatiles), while retaining the benefits of atmospheric pressure operation without MS: small footprint, lightweight, ruggedness, and low cost. This may make FAIMS/IMS attractive for many field applications.

(74) Woods, A. S.; Ugarov, M.; Egan, T.; Koomen, J.; Gillig, K. J.; Fuhrer, K.; Gonin, M.;Schultz, J. A. *Anal. Chem.* **2004**, *76*, 2187.
(75) Jackson, S. N.; Wang, H. Y. J.; Woods, A. S. *J. Am. Soc. Mass Spectrom.* **2005**, *16*, 133.